PHILOSOPHICAL TRANSACTIONS OF THE ROYAL SOCIETY A MATHEMATICAL, PHYSICAL & ENGINEERING SCIENCES

Lunar Gravity Determinations and their Implications

W. L. Sjogren

Phil. Trans. R. Soc. Lond. A 1977 **285**, 219-226
doi: 10.1098/rsta.1977.0058

Phil. Trans. R. Soc. Lond. A. **285**, 219–226 (1977) [219]
Printed in Great Britain

Lunar gravity determinations and their implications†

By W. L. Sjogren
Jet Propulsion Laboratory, Pasadena, California, U.S.A.

[Plates 1 and 2]

The variations in speed of the orbiting Apollo spacecraft as observed from Earth-based radiometric data have provided a direct measure of the local gravitational field. The gravity data were used to infer mass distributions that relate to topography in varying degrees. The mascons exist as mass excesses in topographic lows in all the near-side ringed basins and are best represented as near surface disks with excess loads of 800 kg/cm². Large 100 km size craters like Langrenus, Theophilus, and Copernicus have mass deficits that are consistent with the craters' volumes. Both of these results imply a relatively rigid surface layer that allowed little isostatic adjustment over lunar time. However, the Apennine mountains, presumably formed at the time of the Imbrium impact event, reveal only a small gravitational anomaly compared to their topographic size. This suggests that at this era the Moon was more plastic and isostatically compensated. By using the orbital element history of the subsatellites, the first realistic far-side field has been determined. The far-side ringed basins are mass deficits consistent with the lack of maria filling. The 2 km centre-of-gravity offset from the geometric centre implies a thicker far-side crust that possibly prevented far-side maria flooding. The homogeneity parameter (C/MR^2) is near that of a homogeneous sphere having possibly a small core with a slight density increase towards its centre.

1. Introduction

Lunar gravity information has been acquired from the analysis of radio tracking data (Doppler) obtained from orbiting space vehicles. The dynamical changes in speed as the spacecraft passed over various topographic relief and density variations were measured by Earth-based tracking stations. The accuracy of the system was such that accelerations of 5 mGal (0.05 mm/s²) were resolvable (Sjogren *et al.* 1972*a*). The Apollo landing design provided an optimal geometry situation, because feature resolution is almost directly proportional to the spacecraft altitude. Ten orbits before landing, a low periapsis altitude of 20 km was attained that enabled the collection of detailed gravity observations. There were also excellent data obtained from the two Apollo subsatellites (particles and fields experiments on Subsatellites 1 and 2 of Apollo 15 and Apollo 16, respectively) that nominally had 100 km altitude circular orbits, but due to gravitational perturbations periapsis altitudes of 15–30 km were reached. (The Apollo 16 subsatellite crashed after 35 days, and the battery on Apollo 15 failed after 2 years of orbital operation.)

Before the Apollo missions nothing was known about regional gravity anomalies, and only low-order spherical harmonic terms were available (e.g. J_{20}, C_{22}, C_{31}) (Koziel 1967; Akim 1966). During the Apollo era, but before the first manned landing, new spherical harmonic estimates of the global field were being extracted from the data of Lunar Orbiters I to V

† This paper presents the results of one phase of research carried out at the Jet Propulsion Laboratory, California Institute of Technology, under Contract NAS 7-100, sponsored by the National Aeronautics and Space Administration.

(Tolson & Gapcynski 1968; Lorell 1970; Sjogren 1971; Michael & Blackshear 1972; Liu & Laing 1972). During this same period the mascon discovery (Muller & Sjogren 1968) was made through the analysis of the Lunar Orbiter V radiometric data. Their new approach for reducing these data made the Apollo craft a very attractive instrument for expanding the data set and refining the Lunar Orbiter results.

2. Gravity anomalies

More than 500000 observations have been recorded by Apollos 12–17 and the Apollo 15 and 16 subsatellites. All have been reduced by using the mascon-type analysis of mapping line-of-sight acceleration profiles and contouring them onto topographic maps. Direct correlations with topography are very common. There are a few anomalies that do not correlate with topography, and these may reflect some ancient subsurface structure.

A band from $\pm 30°$ of latitude across the front face of the Moon has been mapped in varying degrees of resolution, depending on spacecraft altitudes. The higher latitude areas ($>30°$) except for Mare Imbrium are poorly determined. For the far side there are no measurements for detailed mappings. This is due to the occultation of the radio signal while the spacecraft is behind the Moon; however, as will be shown later, indirect observations have recently yielded some lower resolution information. A summary of the more prominent near-side gravity features are shown in figure 1, plate 1. These results were compiled from the individual Apollo mission reports (Gottlieb *et al.* 1970; Muller *et al.* 1974; Sjogren *et al.* 1972–1974). There is a great variety of both positive and negative free air anomalies in both highland and maria regions. Each group has its unique characteristics that will be examined in the following subsections.

Mascons

The large positive gravity anomalies over the circular maria basins were verified from the Apollo data, and much more detailed profiles were obtained. Mare Serenitatis was sensed at 15 km spacecraft altitudes rather than 150 km. Mare Humorum was completely covered with some 37 profiles. Mare Crisium and Mare Nectaris were profiled from a 30 km spacecraft altitude. These mascon gravity profiles were modelled using various mass distributions (e.g. a point mass at different depths, several mass points, disks with their top surface at different depths including zero, and several disks at different depths). The process of estimating the best models to match these gravity profiles was done in an iterative least squares reduction. A model was selected and a trajectory with the same geometry as the real orbit was dynamically integrated over the model. This trajectory then produced simulated tracking data that were reduced in the same manner as the raw data. Differencing of the simulated gravity profile (i.e. the theoretical model) with the real gravity profile provided residuals that were used to optimize the modelling parameters (e.g. mass, radius, latitude and longitude of the disk or point mass). The Mare Serenitatis profile is shown in figure 2. The best solution was a surface disk, as was the case for the other mascon profiles. The excess load of 800 kg/cm^2 was nearly the same for all the mascons, except Grimaldi (the mascon with the smallest diameter), which attained more than 1000 kg/cm^2. Evidence that the mascons are not nice symmetric features is shown in figure 2, where definite shoulders are detected in the real data profile. This could imply denser or deeper filling materials produced at various epochs.

How the mascons were formed is still an issue. It does seem, however, that the theory (Stipe

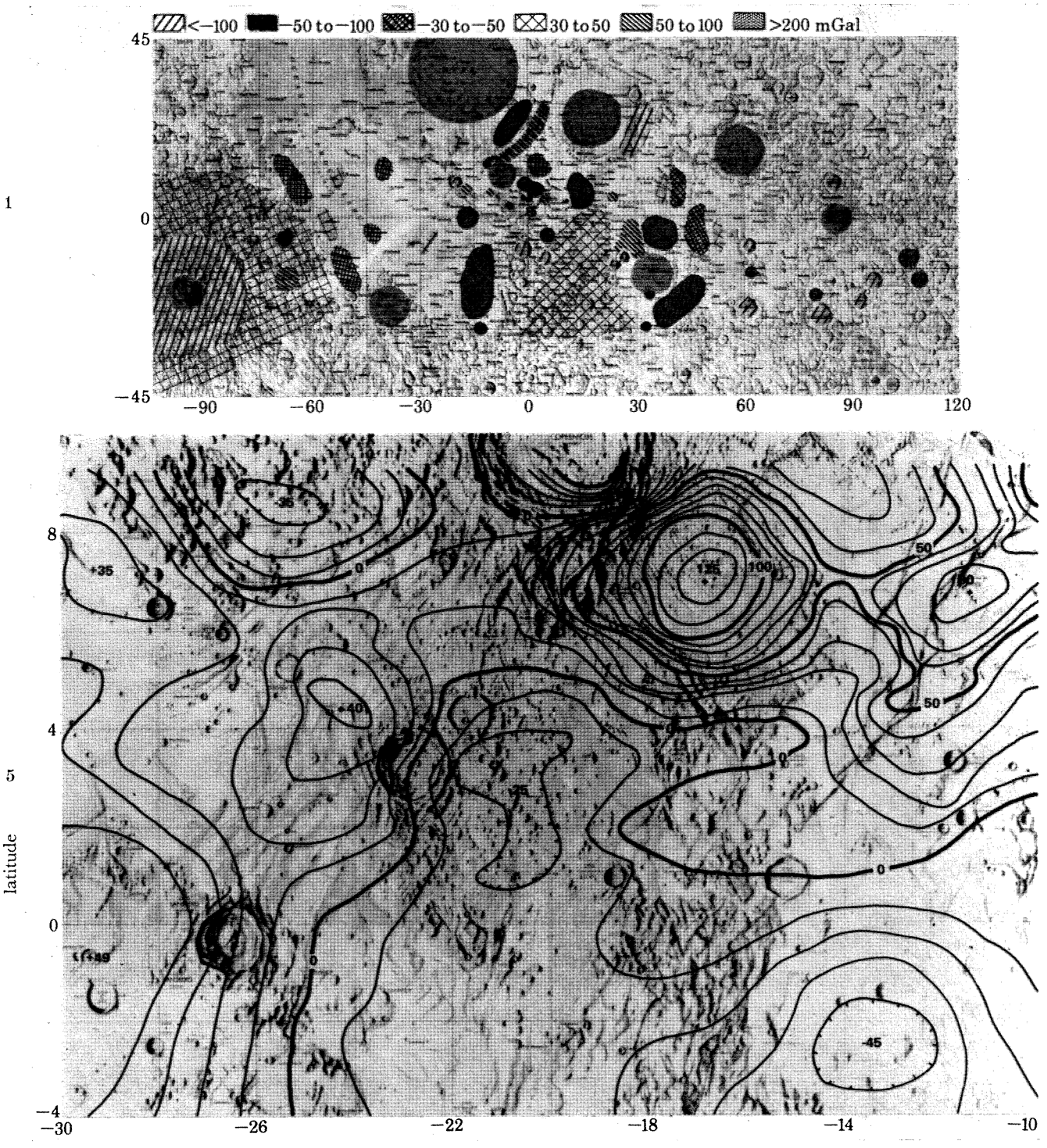

FIGURE 1. Summary of the more prominent gravity anomalies over the lunar near side. *Note:* areas not indicated are between ±30 mGal (primarily irregular maria) or are not yet resolved due to lack of coverage (i.e. large craters like Riccioli).

FIGURE 5. Gravity contours from Apollo 16 subsatellite data (10 mGal contours).

(*Facing p.* 220)

PHILOSOPHICAL TRANSACTIONS OF THE ROYAL SOCIETY A MATHEMATICAL, PHYSICAL & ENGINEERING SCIENCES

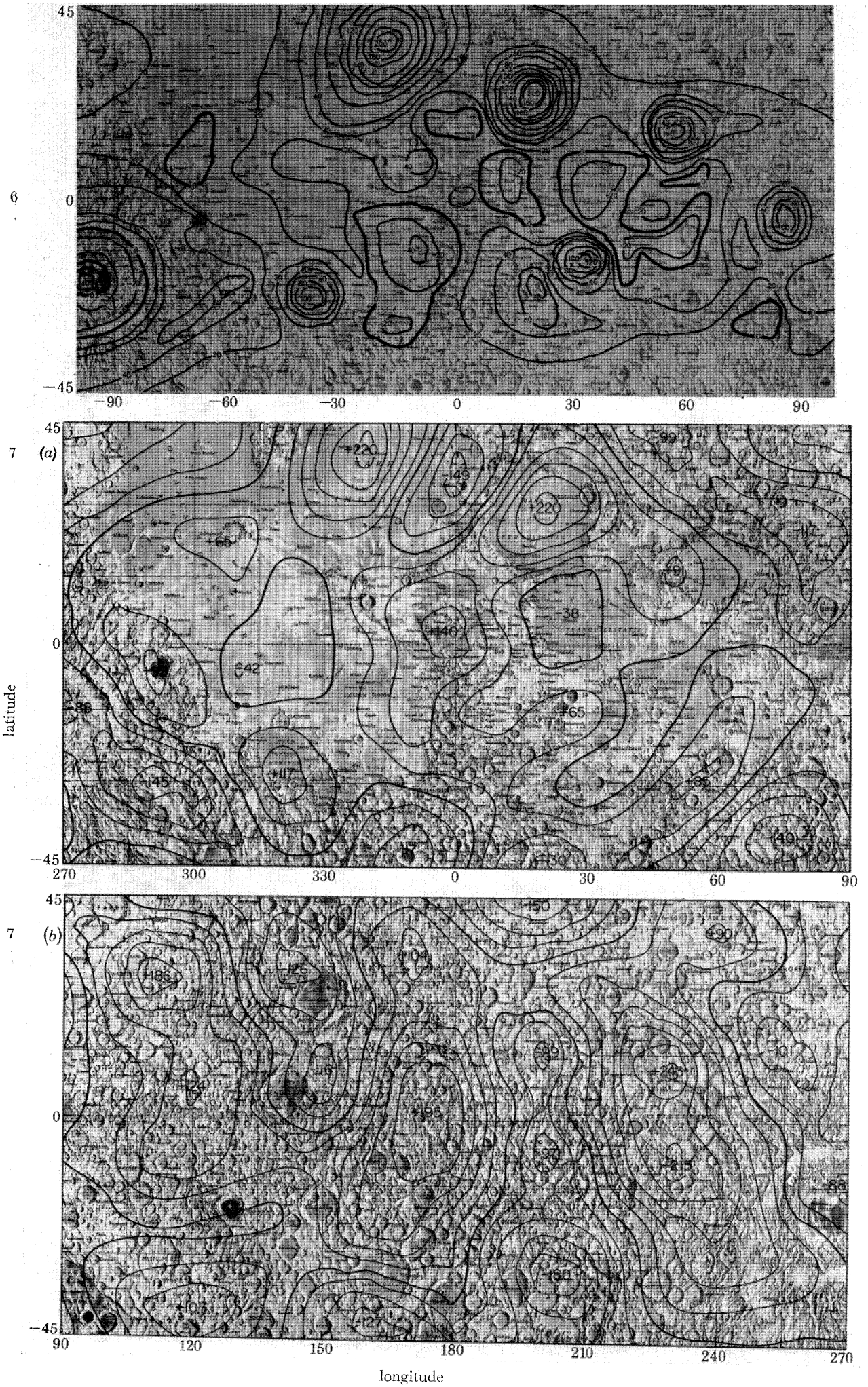

FIGURES 6 AND 7. For description see opposite.

PHILOSOPHICAL TRANSACTIONS OF THE ROYAL SOCIETY A MATHEMATICAL, PHYSICAL & ENGINEERING SCIENCES

1968; Muller & Sjogren 1968) that they are deeply buried remnants of impacting bodies does not model the gravity profile well (figure 2). Numerous theories on the formation of the mascons (Conel & Holstrom 1968; Baldwin 1968; Urey & MacDonald 1971; Phillips *et al.* 1972; Wise & Yates 1970; Kaula 1971; Arkani-Hamed 1973; Wood 1970; Toksoz 1973; Bowin *et al.* 1975; Hulme 1972) have been presented. Many of the theories require a crust thickness of 100 km or more to support the mascons over geologic time. Depth parameters for a two-body mascon as Bowin (1975) proposes are not uniquely determinable with the present data. It is clear that interior model builders (Kaula 1971; Arkani-Hamed 1973; Toksoz 1973; Anderson 1974; Runcorn 1974; Gast 1972) must keep their temperature profiles such that viscosities are high enough to sustain these excess loads for more than 3 Ga. Whether relief on a moho is a realistic model may be forthcoming from a current study of Mare Orientale, which has a large negative gravity ring (figure 1).

Craters

Well over twenty 100 km size craters have been detected (e.g. Ptolemaeus, Hipparchus, Theophilus, Neper, Petavius, Langrenus, Albategnius). They all have large negative anomalies,

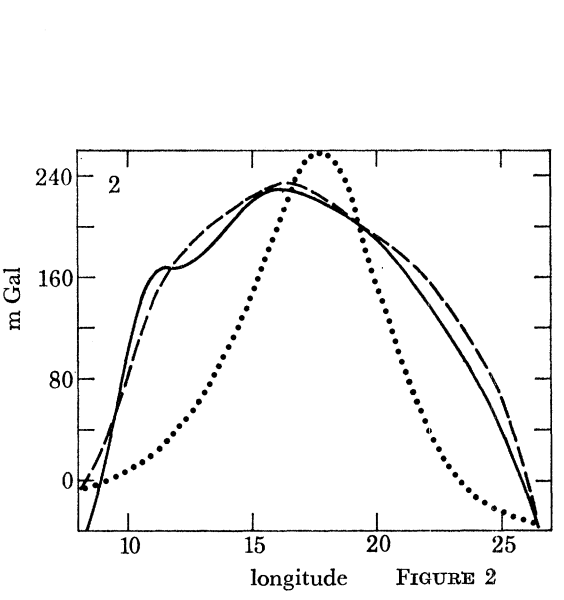

FIGURE 2

FIGURE 3

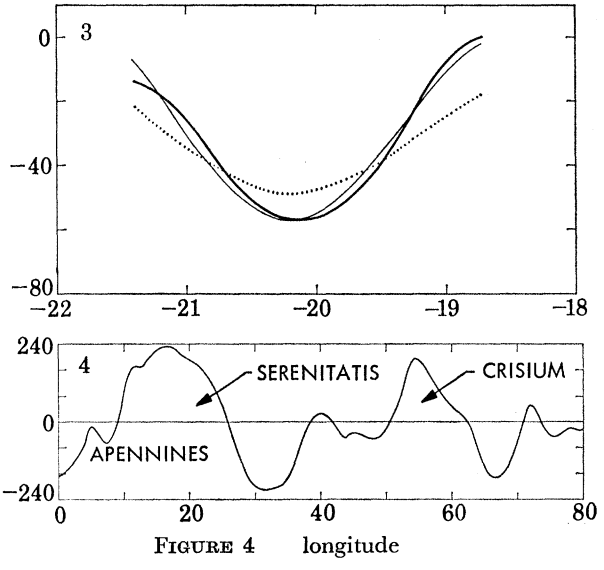

FIGURE 4

FIGURE 2. Mare Serenitatis gravity profile: real data versus simulated data from various models. The solid line indicates real data; dashed line, 245 km surface disk; dotted line, point mass 100 km deep. Both disk and point mass were located at the optical centre of Mare Serenitatis, lat. 26° N, long. 19° E (see Muller *et al.* 1974).

FIGURE 3. Copernicus gravity profile: real data versus simulated data from various models. The heavy line indicates real data; light line, surface disk with rim; dotted line, one surface disk (see Sjogren *et al.* 1974, pp. 41–52, for detailed values).

FIGURE 4. Apollo 15 partial gravity profile from orbit 4.

DESCRIPTION OF PLATE 2

FIGURE 6. Near-side lunar gravity at a 100 km reference altitude from evaluation of 350 surface disks (20 mGal contours) (Sjogren *et al.* 1975).

FIGURE 7. Lunar gravity at a 100 km reference altitude, 16th degree and order spherical harmonics (Ferrari 1975): (*a*) lunar front side, (*b*) lunar far side.

which also shows that the high viscosity of the lunar crust can maintain deficit loadings of 1000 kg/cm². The crater Copernicus was modelled initially with one disk at its optical centre, and it was found that the observed gradients were so large that the rim mass had to be included before reasonable fit (figure 3) could be achieved (Sjogren *et al.* 1974). Once the central mass deficit was determined, a density for the surface material to a depth of 2.3 km was calculated. The density was in excess of the mean density, but given adjustments for map errors and data reduction the value could not be reduced much below 3.0 g cm^{-3}. A similar analysis for the crater Langrenus resulted in a density of 3.05 g cm^{-3}. This indicates that these craters are not in isostatic adjustment and internal stresses require that the Moon be relatively rigid to a depth comparable to the crater size.

Other anomalies

As seen in figure 4 Montes Apenninus (the mountain ridge between Mare Serenitatis and Mare Imbrium) was detected as a small anomaly in comparison to the large Mare Serenitatis anomaly. A preliminary analysis of this feature (Sjogren 1973) indicated that considerable isostatic adjustment has taken place. This would imply that at the time of the Imbrium impact event the lunar crust was relatively plastic (i.e. warmer). More recent work using new topographic ortho-photo maps from the Apollo metric camera system has produced more precise estimates but conclude the same large, isostatic adjustment.

To the east of Mare Serenitatis (long. 30°, lat. 20°) the Apollo 17 landing module (Talwani *et al.*) recorded absolute gravity at several areas near the landing site. An absolute value of 162 694 ± 5 mGal was determined. This is 214 mGal less than what would theoretically have been measured for a homogeneous sphere with radius obtained from the altitude of the landing site. In figure 4 at longitude 30°, there is good agreement with the large 200 mGal negative anomaly (the latitude of the profile is not precisely that of the Apollo site). These negative areas have been proposed (Arkani-Hamed 1973) as possible source regions for mascon material.

The irregular maria have some local variations in gravity but mostly they are mild negative regions. Local positive anomalies within the mare were detected over wrinkle ridge structures, areas with domes, and circular structures (e.g. Lamont in Tranquilitatis, Phillips and Saunders). These have been interpreted to represent possible source areas for intensive maria fill (Scott 1974). In general, the irregular maria exhibit an isostatic condition where the recent maria flooding has been thin compared to circular maria basin fills.

The highlands (South central and those around Mare Orientale) have positive anomalies reflecting the topographic relief. To a first order, they appear to be in isostatic adjustment, consistent with that of an old surface that had low viscosity.

There are several areas where free air gravity features do not correlate with topography. One such area is shown in figure 5, plate 1, just to the southeast of the crater Copernicus where the 125 mGal anomaly was well determined from some 15 orbital tracks. Possibly it is some ancient structure that was obliterated when the Copernicus event occurred.

If one views the lunar front face gravity field from a 100-km reference surface, it appears as shown in figure 6, plate 2 (Sjogren *et al.* 1975). This result was obtained by dynamically reducing some 20 000 raw observations and estimating 350 surface disk masses. Except for anomalies associated with the mascons the other anomalies are ± 40 mGal. These are relatively mild variations and indicate isostasy for most of the Moon. This was first noted by J. O' Keefe (1968) when he inferred that in its early history, the Moon underwent isostatic adjustment much like the Earth does today.

PHILOSOPHICAL TRANSACTIONS OF THE ROYAL SOCIETY A MATHEMATICAL, PHYSICAL & ENGINEERING SCIENCES

Far-side gravity

Our 1975 data analysis has enabled the first reliable gravity map of the far-side to be produced. Previous gravity maps have many disclaimers to their far-side results (Lorell 1970; Michael & Blackshear 1972; Liu & Laing 1972) for even their front-side anomalies showed only weak resemblances to the mascon features. By using the variations of the orbital elements of over a year from the Apollo 15 subsatellite, 35 days of the Apollo 16 subsatellite and some 10 days from Lunar Orbiter V two new gravity solutions have been obtained (Ananda 1975; Ferrari 1975). The agreement between the two entirely different modelling approaches is good. Ferrari's solution of 16th order and degree spherical harmonic expansion is shown in figure 7, plate 2. The free air gravity field is plotted as it would appear at a 100 km altitude in units of milligals. The figure shows how the front-side mascons are resolved, adding confidence that the far-side results are valid. The resolution of the field is approximately 400 km, so precise positioning is hard to obtain. To a first order, one can see that the far-side basins of Korolev, Hertzsprung, Moscoviense, and Mendeleev, are regions of negative anomalies, and the remaining highland areas are broad positives. This again seems to verify that the maria fill of front-side circular basins is the predominant reason for the mascons, since far-side circular basins do not have strong positive anomalies.

3. Radial density variations

The parameter used to describe the internal radial density variations is the homogeneity constant C/MR^2, where C is the polar moment of inertia, M is the mass of the Moon, and R the mean radius. For a value of 0.4 the body is a homogeneous sphere under the assumption of radial symmetry and no density inversions. For a value of 0.67 the body is a hollow sphere. Eckert (1965) proposed the possibility of a hollow Moon to account for the residual in the nodal rate of the Moon's orbit when compared to the theoretical lunar motion. This point was later clarified by T. C. Van Flandern (1968) when it was noted that the time base used was erroneously assumed constant. Our present methods do not use the Moon's orbital motion, but obtain C by combining the results from two other independent experiments that each measure the ratios of moments of inertia.

$$[C/MR^2 = (J_2 + 2C_{22})/\beta].$$

Before the Apollo missions the value of β from physical libration theory was the largest uncertainty in the determination. However, the laser ranging experiment (Williams *et al.* 1973) has obtained the libration parameters so well that it is now the low-order gravity harmonics coefficients, J_{20} and C_{22}, which are the largest uncertainties. These coefficients were not significantly improved with the Apollo data, because the high-frequency gravity variations in the low-altitude orbits corrupted the low-order coefficient solutions. The best determination of the homogeneity constant is 0.395 ± 0.005 (Williams *et al.* 1973). This implies an increase in density towards the centre. Kaula *et al.* (1974) proposes two models that fit this value. The first model has an iron core of 265 km radius and the second model (preferred by Kaula) has a pyroxene mantle (0.4 g cm^{-3} density increase from a crust of 2.95 g cm^{-3}) of 738 km radius with no core at all. In his calculations it was shown that temperature and pressure at depth did affect density and these effects tended to cancel each other.

4. Centre of gravity offset

The offset of the centre of gravity (c.g.) from the centre of the geometrical figure was first measured in the earthward direction by the Ranger probes (Sjogren 1967) and later by radar bounce (Shapiro *et al.* 1968), lunar photometry (Compton & Wells 1969), and landmark tracking (Wollenhaupt *et al.* 1972). The Apollo laser altimeter provided complete 360° profiles at different latitudes and definitely determined the 2 km offset (Sjogren & Wollenhaupt 1973). If one postulates a simple model of a lunar crust overlying denser material where there also exists an offset of the centre of gravity, then a difference in crustal thickness between the far side and near side is all that is required to keep the moments equal to zero. The expression for the crustal thickness difference is

$$\Delta T = 2x\rho/(\rho - \rho_0),$$

where x is the c.g. offset, ρ is the mean density, and ρ_0 is the crustal density. If one assumes a crustal density of 2.94 g cm^{-3} and an offset of 2 km, then the crust thickness difference is 33 km. Since the centre of gravity shift is towards the Earth, this implies that the far-side crust is 33 km thicker than the front-side. Of course, if the crustal density is larger, much thicker crust differences are obtained, as shown in table 1. A direct inference from this is that the thick far-side crust prevented maria flooding which is so predominant on the near side. The shift may actually be caused by some asymmetric cooling (Ransford & Sjogren 1972) or a non-random location of radioactive materials.

Table 1. Difference in crust thickness between near side and far side

($\Delta T = 2x\rho/(\rho - \rho_0)$; $x = 2$ km; $\rho = 3.34$ g cm^{-3})

ρ_0(g cm^{-3})	ΔT/km
2.94	33
3.14	67
3.24	100
3.32	670

5. Circular maria fit

Slightly afield from the present gravity field determination is an interesting result that may reflect an ancient hydrostatic or gravity surface. The Apollo laser altimeter provided very accurate (Sjogren & Wollenhaupt 1973) topographic profiles. These profiles are based on the spacecraft position about the centre of gravity and therefore may not be about the lunar geometric centre. When an offset ellipsoid was determined from 20 circular maria elevations, a very good fit was obtained and the match to another 176 maria points was also good (Sjogren 1975). This is shown in figure 8 where (*a*) shows 196 maria points referenced to the centre of gravity, and (*b*) shows the resulting fit. The group of points near 180° are craters and may not necessarily be valid maria surfaces (they were selected because of the scarcity of any other maria surface). These results suggest the centre of gravity offset is again *ca.* 2.1 km, but in addition the earthward axis (X) is 2.7 km larger than the other equatorial axis (Y). A possible cause may have been gravitational budge effect from an Earth position that was only 1/4 its present lunar distance. However, this leaves unanswered the question of how the centre of gravity shifted from the hydrostatic surface centre to its present location 2 km away.

6. Conclusions

The analysis of free air gravity has provided a measure of lunar isostasy both locally and globally, implying that the Moon was relatively plastic early in its history and that subsequent cooling of the interior has produced a rigid crust that can support loads of 1000 kg/cm². The large impacting bodies that formed the ringed basins are not the primary cause of the mascon anomalies. The maria filling is required, and it is not an even symmetric fill. Most free air gravity anomalies are associated with topography, but those that do not may indicate old

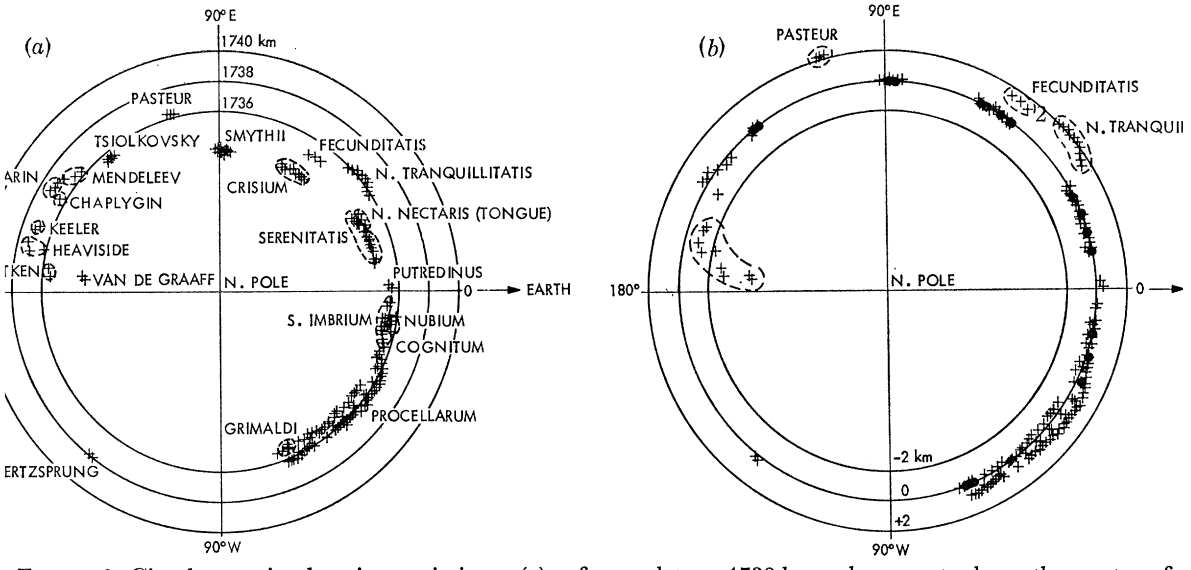

Figure 8. Circular maria elevation variations: (*a*) referenced to a 1738 km sphere centred on the centre of gravity, (*b*) referenced to an offset ellipsoid.

obliterated surface features with subsurface structure. The radial density variations in the Moon are not very large. Two allowable models are: (1) a small 265 km radius iron core, and (2) a more plausible model with a 738 km pyroxene mantle having no core. A crust thickness differential between the lunar near-side and far-side faces could be 33 km or larger. It is proposed that the far-side crust, being thicker, has prevented the extensive maria flooding that is pervasive over the near side. The elevations of the ringed maria surfaces seem to match an ellipsoid model fairly well, and may represent an old hydrostatic surface.

References (Sjogren)

Akim, E. L. 1966 *Dokl. Akad. Nauk. SSR* **170** (4), 799–802.
Ananda, M. P. 1975 *Geochim. cosmochim. Acta* **6** (in the press).
Anderson, D. L. 1974 *Physics Today* **27**, No. 3, 44–49.
Arkani-Hamed, J. 1973 *Geochim. cosmochim. Acta* **4**, 2673–2684.
Baldwin, R. B. 1968 *Science, N.Y.* **162**, 1407–1408.
Bowin, C., Simon, B. & Wollenhaupt, W. R. 1975 *J. geophys. Res.* (in the press).
Compton, H. R. & Wells, W. R. 1969 *NASA TN D*-5231. N.A.S.A. Washington, D.C.
Conel, J. E. & Holstrom, G. B. 1968 *Science, N.Y.* **162**, 1403–1405.
Eckert, W. J. 1965 *Astron. J.* **70**, 787–792.
Ferrari, A. J. 1975 *Science, N.Y.* (in the press).
Gast, P. W. 1972 *The Moon* **5**, 121–148.

Gottlieb, P., Muller, P. M., Sjogren, W. L. & Wollenhaupt, W. R. 1970 *Science, N.Y.* **168**, 477–478.
Hulme, G. 1972 *Nature, Lond.* **238**, 448–450.
Kaula, W. M. 1971 *Phys. Earth Planet. Inter.* **4**, 185–192.
Kaula, W. M., Schubert, G., Lingenfelter, R. E., Sjogren, W. L. & Wollenhaupt, W. R. 1974 *Geochim. cosmochim. Acta* **5**, vol. 3, 3049–3058.
Koziel, K. 1967 *Proc. R. Soc. Lond.* A **296**, 248–253.
Liu, A. S. & Laing, P. A. 1972 *Space Res.* **12**, 163–175.
Lorell, J. 1970 *The Moon* **1**, 190–231.
Michael, W. H. & Blackshear, W. T. 1972 *The Moon* **3**, 388–402.
Muller, P. M. & Sjogren, W. L. 1968 *Science, N.Y.* **161**, 680–684.
Muller, P. M., Sjogren, W. L. & Wollenhaupt, W. R. 1974 *The Moon* **10**, 195–205.
O'Keefe, J. A. 1968 *Science, N.Y.* **162**, 1405–1406.
Phillips, R. J., Conel, J. E., Abbott, E. A., Sjogren, W. L. & Morten, J. B. 1972 *J. geophys. Res.* **77**, 7106–7114.
Phillips, R. J. & Saunders, R. S. 1974 *Proc. 5th Lunar Conf.*, Houston, Texas, 596–597.
Ransford, G. & Sjogren, W. L. 1972 *Nature, Lond.* **238**, 260–262.
Runcorn, S. K. 1974 *Proc. R. Soc. Lond.* A **336**, 11–33.
Scott, D. H. 1974 *Geochim. cosmochim. Acta, Suppl.* 5, 3025–3036.
Shapiro, A., Uliana, E. A., Yapke, B. S. & Knowles, S. H. 1968 *Moon and planets* (ed. A. Dollfus), vol. 2, pp. 34–36.
Sjogren, W. L. 1967 *Measure of the moon* (ed. Kopal & Goudas), pp. 341–342.
Sjogren, W. L. 1971 *J. geophys. Res.* **76**, 7021–7026.
Sjogren, W. L. & Wollenhaupt, W. R. 1975 *The Moon* **15**, 143–154.
Sjogren, W. L., Gottlieb, P., Muller, P. M. & Wollenhaupt, W. R. 1972*a* *Apollo* 15 *Preliminary Science Report*, NASA SP-289, 20.1–20.6. N.A.S.A., Washington, D.C.
Sjogren, W. L., Gottlieb, P., Muller, P. M. & Wollenhaupt, W. R. 1972*b* *Science, N.Y.* **175**, 165–168.
Sjogren, W. L., Muller, P. M., Wong, L. B. & Down, W. 1975 *The Moon* (in the press).
Sjogren, W. L., Wimberly, R. N. & Wollenhaupt, W. R. 1974*a* *The Moon* **9**, 115–128.
Sjogren, W. L., Wimberly, R. N. & Wollenhaupt, W. R. 1974*b* *The Moon* **11**, 35–40.
Sjogren, W. L., Wimberly, R. N. & Wollenhaupt, W. R. 1974*c* *The Moon* **11**, 41–52.
Sjogren, W. L. & Wollenhaupt, W. R. 1973 *The Moon* **8**, 25–32.
Sjogren, W. L. & Wollenhaupt, W. R. 1973 *Science, N.Y.* **179**, 275–278.
Stipe, J. G. 1968 *Science, N.Y.* **162**, 1402–1403.
Talwani, M., Thompson, G., Dent, B., Kahle, H. & Buck, S. 1973 *Apollo* 17 *Preliminary Science Report*, NASA SP-330, 13.1–13.3. N.A.S.A. Washington, D.C.
Toksöz, M. N. & Solomon, S. C. 1973 *The Moon* **7**, 251–278.
Tolson, R. H. & Gapcynski, J. P. 1968 *Moon and Planets* **11**, 3042–3051.
Urey, H. C. & MacDonald, G. J. F. 1971 In *Physics and astronomy of the Moon* (2nd ed.), pp. 213–289. New York: Academic Press.
van Flandern, T. C. 1968 Technical Report 32-1247,13. Jet Propulsion Laboratory, Pasadena, California.
Williams, J. G., Slade, M. A., Eckhardt, D. H. & Kaula, W. M. 1973 *The Moon* **8**, 469–483.
Wise, D. U. & Yates, M. T. 1970 *J. geophys. Res.* **75**, 261–268.
Wollenhaupt, W. R., Osborn, R. K. & Ransford, G. A. 1972 *The Moon* **5**, 149–151.
Wood, J. A. 1970 *J. geophys. Res.* **75**, 6497–6513.

PHILOSOPHICAL TRANSACTIONS OF THE ROYAL SOCIETY A MATHEMATICAL, PHYSICAL & ENGINEERING SCIENCES

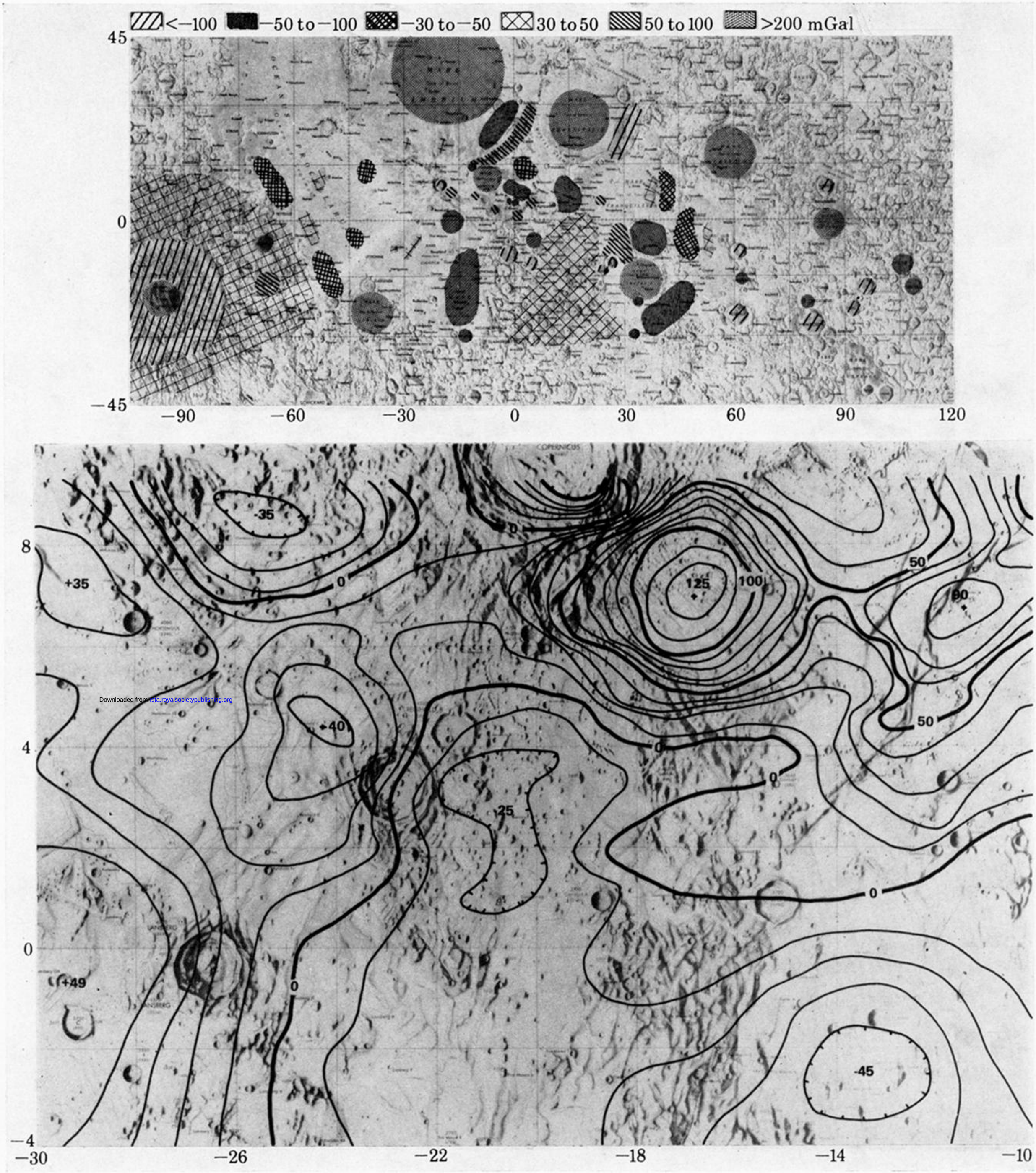

FIGURE 1. Summary of the more prominent gravity anomalies over the lunar near side. *Note:* areas not indicated are between ±30 mGal (primarily irregular maria) or are not yet resolved due to lack of coverage (i.e. large craters like Riccioli).

FIGURE 5. Gravity contours from Apollo 16 subsatellite data (10 mGal contours).

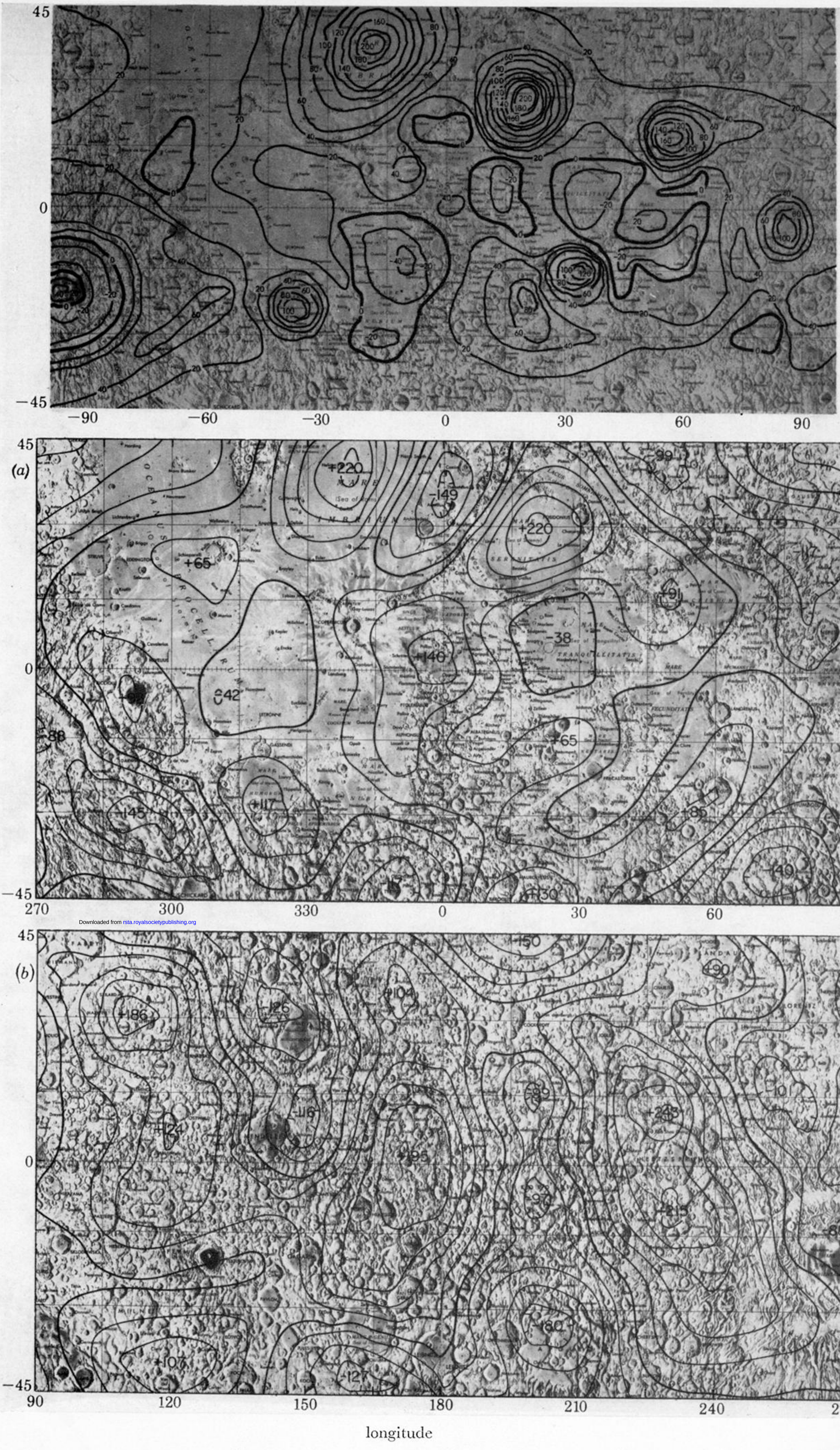

FIGURES 6 AND 7. For description see opposite.